PERGAMON

Vision Research 40 (2000) 3039–3048

Vision Research

www.elsevier.com/locate/visres

# Effect of NADPH on formation and decay of human metarhodopsin III at physiological temperatures

Istvan Szundi [a], James W. Lewis [a], Frederik J.G.M. van Kuijk [b], David S. Kliger *

[a] *Department of Chemistry and Biochemistry, University of California, Santa Cruz, CA 95064, USA*
[b] *Department of Ophthalmology & Visual Sciences, University of Texas Medical Branch, Galveston, TX 77555-1067, USA*

Received 7 February 2000; received in revised form 15 May 2000

**Abstract**

Difference absorption spectra were recorded during the formation and decay of metarhodopsin III after sonicated membrane suspensions of rhodopsin were bleached at 37°C. The data were analyzed using SVD, spectral decomposition and global exponential fitting. By comparison of the results in the presence or absence of 70 μM NADPH and those for bovine or human rhodopsin, a single comprehensive scheme was fit to all the data, including reduction of retinal to retinol by the intrinsic retinol dehydrogenase. On the time scale studied the mechanism involves two 382 nm absorbing species and two 468 nm, absorbing species, supporting the notion that human metarhodopsin III is not a homogeneous species. The results confirm that metarhodopsin III forms and persists sufficiently long in the human retina under physiological conditions that it could undergo secondary photoisomerization. 

*Keywords:* Human rhodopsin; Dark adaptation; Photoregeneration; Retinol dehydrogenase; Metarhodopsin III; NADPH

## 1. Introduction

Organisms contain visual pigments which are optimized by evolutionary processes for the ambient light conditions in which they function. For example, visual pigments of some fish and marine mammals have absorption spectra which are shifted toward the blue relative to the rhodopsins of terrestrial animals in order to take advantage of the predominance of bluer light in the aquatic environment (Archer & Hirano, 1998; Fasick, Cronin, Hunt, & Robinson, 1998). However, continued absorption of light after photoisomerization of a vertebrate visual pigment molecule apparently lacks function, and indeed some of the absorbance changes which occur after initial photoisomerization reduce further absorbance of light. Photointermediates have been detected in vitro which absorb significantly in the visible and which have lifetimes sufficiently long that secondary photoisomerization is possible. Such photoisomerization in vertebrates could either have an undiscovered function (as it does for invertebrates, where secondary photoisomerization can regenerate the visual pigment) or be detrimental under some conditions, so it becomes of interest to determine the degree to which secondary photoisomerization potentially occurs in the human eye.

The most important single factor determining the wavelength of maximum absorbance, $\lambda_{max}$ of visual pigments is the protonation state of the retinylidene Schiff base which binds the vitamin A derived chromophore to a lysine side-chain of opsin. Deprotonation of the Schiff base, which occurs rapidly after photoisomerization and which is obligate for activation, blue-shifts the $\lambda_{max}$ by $\sim 100$ nm. Besides being large, this deprotonation induced blue-shift is remarkable because in the adult human eye it moves the pigment absorbance into a spectral region where the lens is opaque ($\lambda_{max} < 400$ nm). This absorbance change is desirable given that continued absorption of light is likely to cause additional photoisomerization, similar in character to the initial 11-*cis* to all-trans excitation event, but with potentially undesirable consequences. The existence of mutant forms of bovine rhodopsin which are capable of activating the G-protein transducin in their

* Corresponding author. Tel.: +1-831-4592106; fax: +1-831-4594161.
*E-mail address:* kliger@chemistry.ucsc.edu (D.S. Kliger).

0042-6989/00/$ - see front matter 
PII: S0042-6989(00)00148-6

visible absorbing, protonated Schiff base (PSB) form, but which do not occur in nature, indicates that bleaching, in and of itself, may have some operational significance (Zvyaga, Min, Beck, & Sakmar, 1993).

Bleaching under physiological conditions occurs in a few milliseconds and persists for seconds. However, the stable absorption spectrum which prevails during that period is a poor indicator of chemical stability since the retinylidene chromophore (at Lys296 in bovine and human rhodopsin) can hydrolyze to free all-trans-retinal and/or migrate to form Schiff bases with other groups. Since the latter can ultimately protonate and absorb visible light, secondary photochemistry could occur, leading to a variety of possible physiological consequences. This makes it important that these later reactions be understood. Considerable progress has been made in defining the mechanism of Schiff base deprotonation leading up to formation of $R^*$, the form of the metarhodopsin II (meta II) intermediate capable of activating transducin (Hofmann, 1986; Jäger, Szundi, Lewis, Mah, & Kliger, 1998), and hence in defining the initial state for the late reactions. A good deal is also known about the subsequent reactions, particularly for bovine rhodopsin which has been studied extensively (Rotmans, Daemen, & Bonting, 1974; Chabre & Breton, 1979; Blazynski & Ostroy, 1984; Klinger & Braiman, 1992; Davidson, Loewen, & Khorana, 1994), mainly in detergent suspensions substantially below physiological temperatures. Those results provide a qualitative framework for understanding events in the human retina, but quantitative understanding depends on measurements at physiological temperatures in membrane suspensions of human rhodopsin. Time-resolved studies of human rhodopsin have been much more limited, but give clear evidence for the presence of significant amounts of visible absorbing, PSB intermediates in the human retina (Ripps & Weale, 1969; Alpern, 1971; Baumann & Bender, 1973; Crescitelli, 1985).

We have characterized the late reactions using rhodopsin prepared from human donor eyes previously used for corneal transplants (Lewis, van Kuijk, Carruthers, & Kliger, 1997). That study, which used global fitting of time-resolved difference spectra, showed that in the absence of reduction of all-trans-retinal an even larger fraction of late PSB intermediates formed after photoexcitation of human rhodopsin compared to what was seen for bovine rhodopsin. Here we extend that work to reactions in the presence of NADPH, the cofactor for reduction of retinal by the endogenous retinol dehydrogenase (Wald & Hubbard, 1949; Lion, Rotmans, Daemen, & Bonting, 1975; Palczewski et al., 1994). By comparison of kinetics in the presence and absence of NADPH, a general reaction scheme was deduced for bovine and human rhodopsin late intermediates. Besides its significance for understanding secondary photochemistry in the human retina, the late intermediates are of interest because they have been proposed to be involved in a mechanism accounting for dark adaptation (Leibrock, Reuter, & Lamb, 1998).

## 2. Methods

Human ROS were prepared using a sucrose density gradient, floatation method (van Kuijk, Buck, Lewis, & Kliger, 1993) from donor eyes provided by the Montana Eye Bank, Missoula, MT. Extrinsic membrane proteins were removed by hypotonic washing with pH 7.0, 1 mM EDTA solution, and after resuspension of the final pellet in TBS buffer (60 mm KCl, 30 mM NaCl, 2 mM $MgCl_2$, 0.1 mM EDTA, 10 mM tris(hydroxymethyl)aminomethane, pH 7.0), the solution was sonicated to reduce turbidity as described previously (Lewis et al., 1997). Hypotonically washed membrane suspensions of bovine rhodopsin were prepared (Thorgeirsson, Lewis, Wallace-Williams, & Kliger, 1993) and sonicated similarly. Final concentration of rhodopsin in these solutions ranged from 28 to 31 μM as determined spectrophotometrically after 1:10 dilution in 1% ammonyx LO detergent.

A Hewlett-Packard (Palo Alto, CA) 8452 photodiode array spectrophotometer was used to measure time dependent absorption spectra of membrane suspension samples. Two issues must be addressed regarding these measurements. First, even after sonication and dilution of samples as described below, substantial turbidity existed. Therefore, technically what was reported by the HP-8452 was not absorbance (i.e. beam attenuation due to absorption alone), but was the device dependent property extinction (beam attenuation due to absorption and light scattering). Since effects of absorption and light scattering are additive, absorbance can be determined from extinction by subtracting out the component due to light scattering. The second issue regarding measurements on visual pigment samples with the HP-8452 is the possibility of actinic effects by the probe beam. These can be reduced by shortening the exposure time for each spectrum from the 1 s default value and by using a suitably chosen color filter to attenuate the most actinic wavelengths in the probe beam before it reaches the sample. Here an integration time of 0.4 s was selected and a Roscolux (Rosco, Port Chester, NY) Salmon Pink filter was used. This filter is similar to the Hoya M-10 filter used previously (Lewis et al., 1997) but performed better because it transmitted more light in the region to the red of 540 nm, yielding higher signal-to-noise (S/N) ratio measurements in that portion of the spectrum.

Measurements were performed in a 1 cm path length, semimicro cuvette (total volume 1 ml) which was masked to confine the spectrophotometer probe beam

to the sample volume. For measurements on bovine rhodopsin a 200 μl aliquot of sonicated solution was added to 800 μl of TBS. Since the human rhodopsin suspensions were more turbid, measurements were made using 150 μl aliquots of the sonicated solution diluted into 850 μl TBS. The maximum extinction occurred for human rhodopsin at 300 nm (the shortest wavelength monitored) and the average extinction value there was 1.83. For kinetic measurements of the bleaching sequence including reduction of all-trans-retinal to retinol, sufficient NADPH stock solution was added to the TBS in the cuvette to produce a final concentration of 70 μM. After all additions were made, the sample was equilibrated in the cuvette holder of the HP-8452 at 37°C for 20 min prior to recording the prebleach spectrum. The sample was then bleached using a 30 s exposure to the fiber optically coupled output of a Cole-Parmer (Chicago, IL) microscope fulminator equipped with a Coming (Coming, NY) 3-71 yellow filter, and a series of 40 spectra were collected at 30 s intervals. After completion of these scans, sufficient 0.5 M NH20H stock (prepared in TBS and pH adjusted to 7.0) was added to produce a final concentration of 20 mM and the sample was rescanned. The sample was then exposed to the bleaching lamp for 1 min and rescanned again. The position of the minimum in the bleaching (negative) region of this final difference spectrum is blue-shifted if isorhodopsin (9-*cis* chromophore) is formed during the initial bleach, and as reported previously (Lewis et al., 1997) there was no evidence seen here for isorhodopsin formation at this temperature.

The time-dependent difference spectra collected at uniform time intervals are not optimum for exponential fitting since a disproportionately large number of spectra are then collected at late times when kinetic changes have decayed. To improve this situation, after the first ten spectra, later spectra were grouped to simulate a logarithmic time base. As previously noted (Lewis et al., 1997), the raw data contained small absorbance offsets as well as a steady increase in light scattering with time. The spectral shape of the light scattering was determined from the extinction spectrum of an unbleached sample, where prior to photoexcitation the time dependent change was entirely due to light scattering changes, and closely followed a $1/\lambda^2$ dependence. The contributions due to offsets and light scattering drift could be estimated from the data in the far red end of the spectra (near 700 nm) and were subtracted from the raw data before fitting. The kinetic analysis is based on the assumption that the chemical processes are first order reactions, and thus the time dependence of the changes involved can be represented by exponential functions. Fitting of exponential functions to the experimental data can be carried out more efficiently if singular value decomposition (SVD) is performed on the data prior to the fitting procedure (Shrager & Hendler, 1982; Hendler & Shrager, 1994). SVD transforms the data matrix, **A**, into three component matrices: $\mathbf{A} = \mathbf{U} \cdot \mathbf{S} \cdot \mathbf{V}^{\dagger}$. Basis spectra, **U**, have the property of being orthogonal and being ordered according to their significance value contained in **S**, so that the first basis spectrum contains the largest contribution from time dependent changes (signal) and the last contains the least time-correlated information (noise). The time dependence of the basis spectra are given in **V** which can be fit with exponentials. By omitting some of the less-time correlated basis spectra from exponential fitting, noise levels can be reduced, making exponential fits more stable. Even if the noise reduction option is not exercised, SVD speeds fitting by dramatically reducing the number of parameters which must be optimized when data is fit to a sum of exponential decays (Hug, Lewis, Einterz, Thorgeirsson, & Kliger, 1990), and as described below, the basis spectra can be useful for determining how many intermediate species are present. Exponential fitting yields a time constant and spectral shape (b-spectrum) for each exponential component as well as a time-independent b-spectrum, $b_0$, which corresponds to the spectral change extrapolated to very long times. The **V** matrix produced by SVD of the experimental data was fit to the largest number of time constants which could be reproducibly fit to the data. In all cases, fits with fewer exponentials than the number reported resulted in noticeably poorer residuals.

The results of exponential fitting of the data are general, i.e. independent of any mechanistic assumption except that all processes are first order or at least pseudo first order. Methods described previously (Szundi, Lewis, & Kliger, 1997) were used to extend the analysis and determine a kinetic scheme or mechanism which could account for the data. Here an important constraint on candidate mechanisms is the fact that the same steps which take place in the absence of NADPH must take place in its presence along with an additional retinal reduction step. However, even taking advantage of the high degree of overlap between mechanisms prevailing with and without NADPH (and also presumably between bovine and human), special difficulties arise here because of S/N limits on the number of exponentials which can stably be fit to the data. This is particularly a problem for late rhodopsin photointermediates because a variety of species can and do form after Schiff base hydrolysis. Given the complexity of meta-II decay, it is likely that one or more of the observed rates could result from degeneracy or at least apparent degeneracy of rates in a mechanism nominally justifying more exponential components than the number fit. Kinetic spectral data have a clear advantage (as compared to single wavelength kinetic data) in resolution of such degeneracy since the existence of

degeneracy can be revealed by the presence of 'extra' intermediate spectra, beyond the minimum number required to account for the number of exponentials fit. The need for extra intermediates can in principal be determined by fitting the b-spectra using the spectral shapes of intermediates as described previously (Szundi et al., 1997), but in practice, as shown below, they are sometimes more easily determined from fitting the basis spectra resulting from SVD since these also are required to be linear combinations of F$\varepsilon$, the intermediate spectra: $\mathbf{U} = \boldsymbol{\varepsilon} \cdot \mathbf{Q}$. The data matrix thus becomes: $\mathbf{A} = \boldsymbol{\varepsilon} \cdot \mathbf{Q} \cdot \mathbf{S} \cdot \mathbf{V}^{\dagger}$ The composition matrix, $\mathbf{Q}$, combined with $\mathbf{S}$ and $\mathbf{V}$ gives the time dependent concentrations of the spectral intermediates: $\mathbf{C} = \mathbf{Q} \cdot \mathbf{S} \cdot \mathbf{V}^{\dagger}$. Note that the spectral intermediates whose concentrations are described in $\mathbf{C}$ may represent either a single kinetic intermediate form (i.e. a homogeneous intermediate) or a number of isospectral intermediates evolving on different time scales.

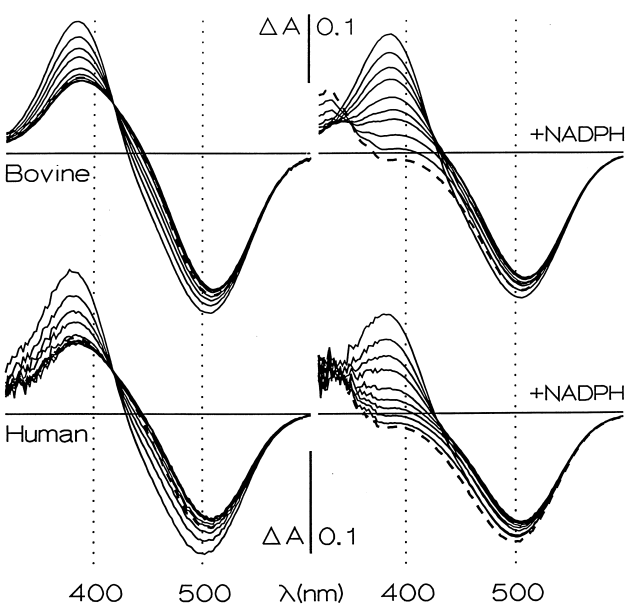


Fig. 1. Difference absorption spectra recorded after photoexcitation of sonicated membrane suspensions of rhodopsin at 37°C. The first spectrum, which shows the largest positive difference at 380 nm and largest negative trough near 500 nm, was recorded 45 s after the beginning of a 30 s light exposure. Subsequent difference spectra were collected every 30 s for 20 min. Overlapping of spectra occurs because the changes at the later times are small, and consequently only a subset of the data collected is shown here. Spectra shown represent data at 45, 75, 105, 135, 195, 255, 315, 465, 720, 1140 s. The last six spectra are averages of several spectra and the final spectrum is shown as a dashed line. Samples yielding spectra on the right contained 70 μM NADPH, the cofactor for endogenous retinol dehydrogenase.

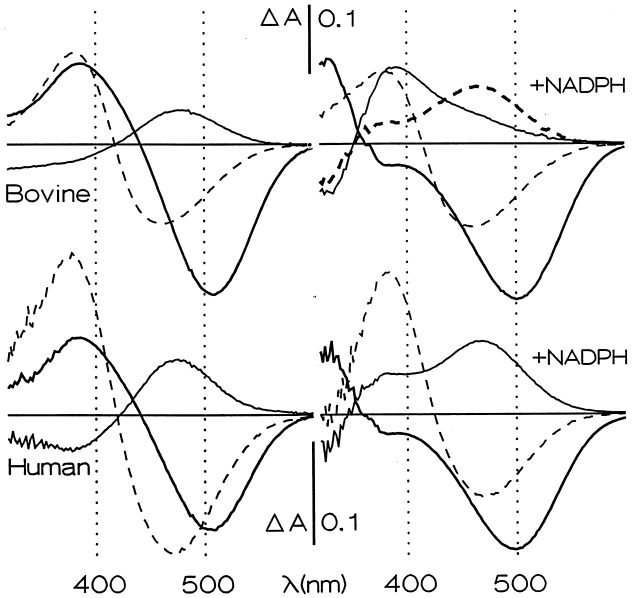


Fig. 2. Spectral changes (b-spectra) associated with the time constants obtained by global fitting. The data in Fig. 1 were simultaneously fit at all wavelengths to a sum of exponential decays. The upper left panel shows the spectral changes associated with the two base e time constants, 110 and 1130 s, obtained for bovine rhodopsin as the dashed and light curves, respectively. The time independent component ($b_0$) is shown as the heavy curve. The relation between the raw data and the b-spectra is a simple one in that the sum of all the b-spectra represents the fit's reconstruction of data which would hypothetically be obtained immediately after photoexcitation. As time progresses the faster b-spectra disappear from the corresponding data until at a hypothetical infinite time only $b_0$ is left. Similar curve styles are used in the other panels to show the spectral components associated with the 98 and 350 s components fit to the data for human rhodopsin and 93 and 510 s components fit to data for human rhodopsin with NADPH. For bovine rhodopsin with NADPH three exponentials could be fit to the data with decay times 105 and 375 s in the curve styles of the other panels and a 1695 s component shown as the dashed heavy line.

## 3. Results

Time dependent absorption difference spectra collected after rhodopsin photoexcitation are shown in Fig. 1 (for clarity, only a subset of the data are shown). Global fitting of the data to sums of exponential decays yielded the b-spectra shown in Fig. 2, with the corresponding time constants (base e) given in the caption to the figure. Two exponentials best fit the data except for bovine rhodopsin in the presence of NADPH where a three exponential fit gave a significant improvement in residuals over a two exponential fit. The small number of exponentials found should not be taken as evidence that a simple mechanism prevails since data collected with and without NADPH are not consistent with analysis in terms of the simplest kinetic schemes associated with two and three rates. In principle, where only two observed rates are found, as few as three intermediate species may be present. However, it is well known

that more intermediates may participate in a larger reaction scheme if it is a degenerate one, i.e. if some of the rate constants in the larger reaction scheme combine to yield apparent rates which are identical or which appear identical within the $S/N$ ratio experimentally achievable. Conventional kinetic analysis routinely excludes degeneracy from consideration unless objective support can be produced for it.

Direct evidence for degeneracy in the case of our data comes from decomposition of the basis spectra in terms of a minimum number of intermediate spectra which have characteristics typical of visual pigment intermediates (Szundi et al., 1997; Nagle, Parodi, & Lozier, 1982). The fits to the basis spectra using the intermediate spectra from Table 1 are shown in Fig. 3 for bovine rhodopsin and in Fig. 4 for human rhodopsin. Table 1 contains the $\lambda_{max}$ values and the relative extinction coefficients of the intermediate and unbleached pigment spectra required to fit our basis spectra. A spectral component with $\lambda_{max} = 348$ nm, required in the fit, was assigned to NADPH and was combined with the 328 nm spectrum. In general four intermediate spectra were required, and temporal profiles of the contributions of the intermediate spectra are shown below the fits to the basis spectra in Figs. 3 and 4. The temporal profiles of the intermediates could also be reproduced by directly fitting the data after adding back the spectrum of the bleached visual pigment. The small variation in the amplitude of the bleach component is close to the noise level of the experiment and may well be due to allowing it to be adjusted in the fitting process. Similarly, in the case of the samples without NADPH, reduction of all-trans-retinal to retinol is not expected, and so the small variations in the 328 nm absorbing component may result from noise in the data. Since both these variations likely result from noise or from experimental drifts not related to rhodopsin photochemistry, their contributions were removed in further analysis. Even after these contributions are removed, however, it is clear that four spectral intermediates participate in the complete kinetic scheme for the late processes of human rhodopsin, where only two exponential decays are detected, and hence fitting

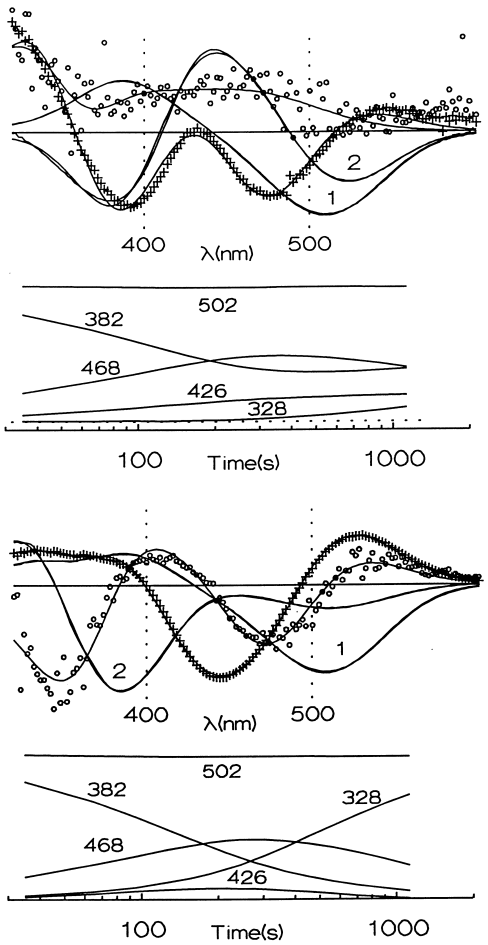


Fig. 3. Fit of intermediates to basis spectra obtained from SVD of bovine rhodopsin data. (Top panel) Shown are the first four basis spectra for bovine rhodopsin without NADPH (labeled curves show basis spectra 1 and 2; points +, ○ show basis spectra 3 and 4, respectively). Smooth curves show the fit obtained to the basis spectra using the intermediates whose characteristics are given in Table 1. The plot below the basis spectra gives the temporal behavior of the spectral intermediates obtained by fitting the data. Each temporal curve is labeled with the $\lambda_{max}$ of the intermediate which it describes. The curve labeled 502 shows the amplitude of the pigment prior to bleaching which went to form the other intermediates which are plotted. The dotted line shows the zero level of the intermediate concentrations. (Bottom panel) Shown are the first four basis spectra for bovine rhodopsin with 70 μM NADPH added and the temporal profile of the intermediates (curves are labeled as described for the top panel).

Table 1
Intermediate spectral forms from decomposition of basis spectra

| | | | | | |
|---|---|---|---|---|---|
| *Bovine* | | | | | |
| $\lambda_{max}$ (nm) | 502 | 468 | 426 | 382 | 328[a] |
| Relative amplitude | 1 | 0.7 | 1.0 | 1.05 | 0.76 |
| *Human* | | | | | |
| $\lambda_{max}$ (nm) | 499 | 468 | 426 | 382[a] | 328[a] |
| Relative amplitude | 1 | 0.9 | 1.0 | 1.2 | 0.76 |

[a] The 328 nm absorbing component (all-trans-retinol) appears as NADPH is consumed and consequently the 348 nm absorbance of NADPH is combined into this component.

of the basis spectra gives evidence for a primary degeneracy in the observed rates.

Besides this primary degeneracy as evidenced by the need for at least one extra spectral form, we also found evidence for a secondary degeneracy in the form of isochromic species which differ chemically in having different reaction rates. Therefore the species listed in Table 1 are not necessarily chemically homogeneous. The evidence for this type of degeneracy comes primarily from the time dependence of intermediate concentrations in the absence of NADPH (Figs. 3 and 4) and

from the b-spectra of bovine rhodopsin in the presence of NADPH (Fig. 2). The concentration time dependence in the absence of NADPH shows the conversion of the initial 382 nm form to a 468 nm form. After reaching its maximal level, the 468 nm form converts to a 382 nm form at later times and sets up a final equilibrium which favors the 382 nm form over the 468 nm form. This kind of time dependence cannot be reconciled with the presence of only one 382 nm and one 468 nm kinetic form. The second and third b-spectra of bovine rhodopsin in the presence of NADPH indicate the reduction of retinal (as shown by the negative lobe at 328 nm). The main decaying components (positive lobes) in the two b-spectra are the same 382 and 468 nm spectral forms but in very different ratios. These two b-spectra suggest that two 468 nm kinetic forms are present in the reaction mechanism. The presence of the 382 nm form in the positive lobes of all three b-spectra indicates one early and one late isospectral, 382 nm intermediate form, with the latter one being reduced by NADPH.

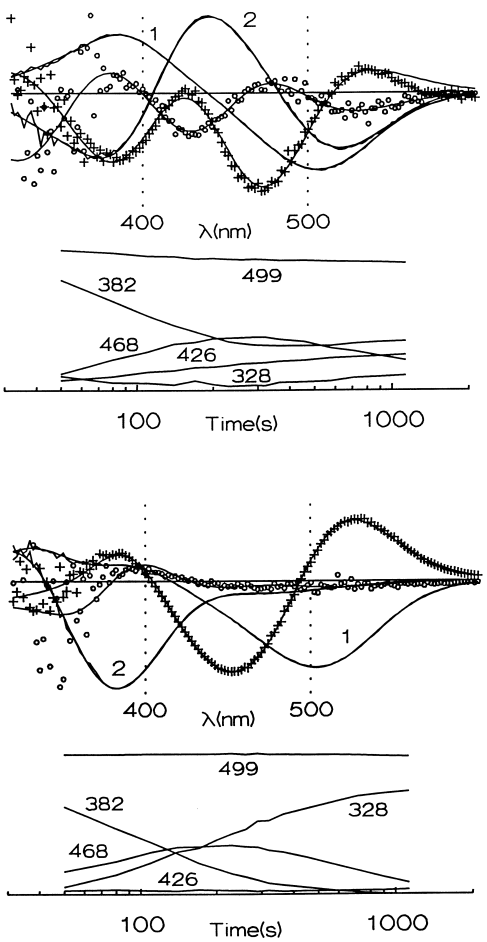


Fig. 4. Fit of intermediates to basis spectra obtained from SVD of human rhodopsin data. (Top panel) Shown are the first four basis spectra for human rhodopsin without NADPH (labeled curves show basis spectra 1 and 2; points +, ○ show basis spectra 3 and 4, respectively). Smooth curves show the fit obtained to the basis spectra using the intermediates whose characteristics are given in Table 1. The plot below the basis spectra gives the temporal behavior of the spectral intermediates obtained by fitting the data. Each curve is labeled with the $\lambda_{max}$ of the intermediate which it describes. The curve labeled 499 shows the amplitude of the bleached pigment which went to form the other intermediates which are plotted. (Bottom panel) Shown are the first four basis spectra for human rhodopsin with 70 μM NADPH added (curves are labeled as described for the top panel).

Based on these features of the concentration time dependence and b-spectra, the following basic elements need to be incorporated into the kinetic scheme. The reaction scheme should start with the conversion of the early 382 nm form to a 468 and 426 nm form, and to a late, isospectral 382 nm form. The late 382 nm form should be in equilibrium with the 426 nm form and a late 468 nm form. Both the early and late 468 nm forms should be connected to the 382 nm form which undergoes the reduction step. Within these constraints, the best fit to the data for both bovine and human rhodopsin in the presence and absence of NADPH was obtained using the following scheme:

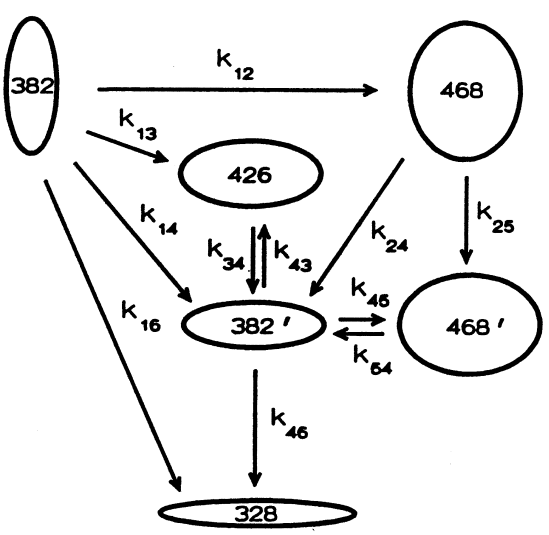


Because of the presence of isospectral intermediates and the number of reaction steps in the scheme, some of the b-spectra calculated from the kinetic matrix show similar shapes and/or small amplitudes. As described above, this results in several of these processes appearing to be degenerate within the signal to noise level constraints of the data, and Fig. 5 illustrates how the various degenerate (or quasi-degenerate) processes combined to give the observed b-spectra in the case of bovine rhodopsin without NADPH. Table 2 gives the values of rate constants which were determined from fitting this scheme to the data. Figs. 6 and 7 show the temporal behavior of the concentrations of the species which participate in the scheme.

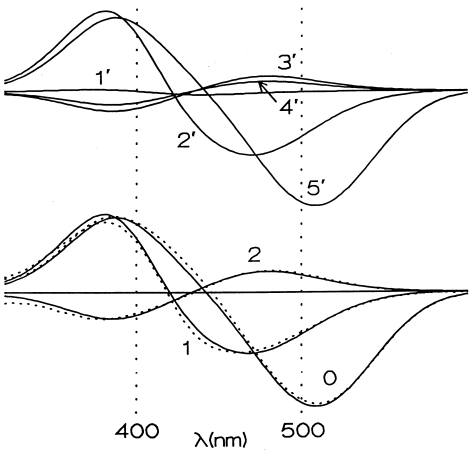


Fig. 5. Example of how quasi-degenerate processes combine to yield the apparent lifetimes observed for bovine rhodopsin without NADPH. The upper panel shows the b-spectra associated with the four exponential lifetimes (60, 107, 417 and 1165 s) which result from the proposed scheme using the rate constants shown in Table 2. The numbers labeling these quasi-degenerate processes are primed to distinguish them from the unprimed numbers which are used to denote the processes actually observed. As shown in the lower panel, the model b-spectra 1′ and 2′ combine with part of 3′ to account for the fastest observed lifetime (110 s), giving the fit to $b_1$ shown by the dotted line. The second observed b-spectrum, $b_2$, associated with the 1130 s decay time results from the remainder of 3′ (70%) which combines with 4′ to produce the fit shown by the dotted line.

Table 2
Microscopic rate constants determined for bovine and human rhodopsin

| | Bovine ($s^{-1} \times 10^3$) | Human ($s^{-1} \times 10^3$) |
|---|---|---|
| $k_{12}$ | 5.3 | 5 |
| $k_{13}$ | 1.2 | 2 |
| $k_{14}$ | 2.8 | 1.6 |
| $k_{16}$ | 0.3 | 1.6 |
| $k_{25}$ | 1.4 | 4.0 |
| $k_{24}$ | 1.0 | 2.2 |
| $k_{34}$ | 12 | 12 |
| $k_{43}$ | 4.5 | 7.2 |
| $k_{45}$ | 0.4 | 1.4 |
| $k_{54}$ | 0.6 | 2.2 |
| $k_{46}$ | 7 | 20 |

## 4. Discussion

We propose a single scheme to describe late rhodopsin intermediates under all the conditions we studied. The microscopic rate constants in the scheme were optimized to reproduce the intermediate concentration time dependences and the experimental b-spectra in the presence and absence of NADPH. In the optimization procedure concentrations of the isospectral intermediates calculated from the kinetic matrix were combined into single components. The final 328 nm absorbing product is retinol, and the processes producing it do not occur in the absence of NADPH. The initial 382 nm absorbing species may either be meta II or an early decay product of meta II. There is evidence for proton release (Bennett, 1980) and partial receptor based deactivation (Baylor & Burns, 1999) on the few second time scale following excitation which indicates that our measurements begin with the initial product of meta II decay. The fact that slow production of retinol ($k_{16}$) takes place in the presence of NADPH indicates the 382 intermediate involves retinal in some restricted form. However, the fact that a later, much more rapid reduction can occur ($k_{46}$) shows that the initial 382 nm absorbing species should not be identified with free all-trans-retinal, which must be the second 382 nm, absorbing product, 382′.

Decay products of meta II have been proposed to be responsible for the elevated threshold for excitation of rod cells observed after rhodopsin is bleached. Two components of this elevated threshold have been identified, one involving limited back reaction to the active form, meta II, and the other arising from weak direct

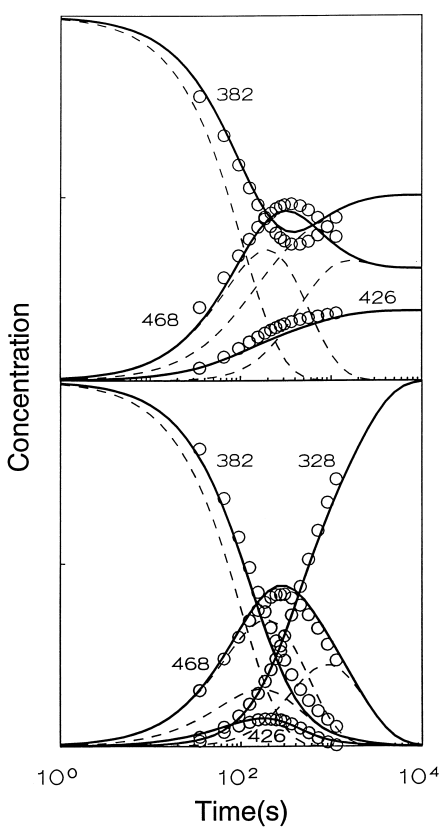


Fig. 6. Concentration of intermediates after photoexcitation of bovine rhodopsin. Circles show concentrations deduced from fitting the basis spectra to intermediate spectra and expressing each time dependent difference spectrum in terms of the basis spectra. The solid lines show the fit to these data obtained using the mechanism shown in the text. In the case of the isochromic intermediates dashed lines show the contributions of the individual components. (Top panel) Bovine rhodopsin without NADPH (Bottom panel) Bovine rhodopsin with 70 μM NADPH.

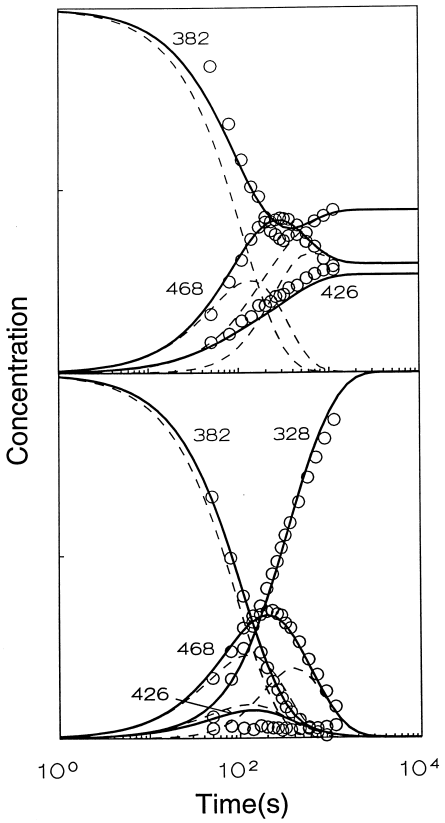


Fig. 7. Concentration of intermediates after photoexcitation of human rhodopsin. Circles show concentrations deduced from fitting the basis spectra to intermediate spectra and expressing each time dependent difference spectrum in terms of the basis spectra. The solid lines show the fit to these data obtained using the mechanism shown in the text. In the case of the isochromic intermediates dashed lines show the contributions of the individual components. (Top panel) Human rhodopsin without NADPH. (Bottom panel) Human rhodopsin with 70 μM NADPH.

activation of transducin by the complex of phosphorylated rhodopsin and arrestin (Hofmann, Pulvermüller, BuczyIko, Van Hooser, & Palczewski, 1992; Leibrock et al., 1998). Our results do not preclude the existence of the required backward path to meta II since the extent apparently needed is quite small and likely to be below the precision limit of our measurements. Conclusions regarding the second component are complicated by the fact that our stripped preparations do not contain arrestin or rhodopsin kinase. However, we note that the time constant for decay of the so called second component of dark adaptation is approximately 2 min (Lamb, 1981) which is similar to the time constant we observe for retinol production. It thus seems possible that removal of all-trans-retinal (and intermediates coupled to it by equilibria) accounts for decay of the second phase of dark adaptation.

The fact that two distinct species absorbing at 468 nm occur in the mechanism is consistent with previous work documenting the heterogeneous chemical nature of the bovine meta Ill intermediate (van Breugel, Bovee-Geurts, Bonting, & Daemen, 1979). That work showed the long wavelength absorbing species to be principally protein-bound retinal with smaller quantities of retinylidene-phosphatidylethanolamine. In keeping with the usage there we refer here to the mixture of 468 nm absorbing species as meta III. Regarding the relative significance of meta III in the human retina versus bovine, the concentration profiles in Figs. 6 and 7 show smaller, but still substantial amounts of meta III forming after photoexcitation of human rhodopsin compared to bovine. However, as shown in Table 1, the extinction coefficient of human meta III is at least 20% larger than that of bovine meta III, accounting for the fact that in the absence of NADPH human rhodopsin develops more 468 nm absorbance than does bovine rhodopsin (Lewis et al., 1997). In the presence of NADPH a larger disparity exists between the human and bovine concentrations of 468 nm absorber which results from the fact that the human retinol dehydrogenase displays more activity than the bovine form. This difference in activity is clearly seen in the raw data and accounts for the larger difference in the 460 nm region between the right and left sides of the bottom of Fig. 1 compared to the difference caused by NADPH in the bovine data at the top. In spite of the increased activity of human retinol dehydrogenase compared to bovine, the data in Fig. 7 show that even with the increased activity NADPH does not dramatically reduce the meta III concentration except at the longest times (several minutes). Therefore it is likely that after large bleaches substantial concentrations of meta III can form in vivo and persist for minutes.

The mechanism we propose is an expanded version of the one previously found to describe formation and decay of metarhodopsin III in the perfused human retina (Baumann & Bender, 1973). Extensions here include the inclusion of a 426 nm absorber and the 468′ intermediate, and as can be seen in Fig. 7, their participation is most evident in data collected in the absence of NADPH, a condition inaccessible to perfused retina studies. Our inclusion of a shorter wavelength PSB intermediate absorbing at 426 nm is similar to the results of Blazynski and Ostroy (1984) who found a 440 nm absorbing PSB form of *n*-retinyl opsin (NRO) and a meta $III_{465}$ intermediate after photoexcitation of solubilized bovine rhodopsin at low temperatures. For the decay of the initial human 382 nm absorber, Baumann and Bender (1973) report a rate constant of $9 \times 10^{-3}$ $s^{-1}$ which agrees well with the sum of our $k_{12}$, $k_{13}$ and $k_{16}$, $8.6 \times 10^{-3}$ $s^{-1}$. The value they deduce for the rate of retinal reduction to retinol, $3 \times 10^{-2}$ $s^{-1}$, is higher than our $k_{46}$, but their data showed considerable uncertainty in that rate, so their result is in reasonable agreement with what we report. Even the smaller value we report is three times the rate seen for bovine

rhodopsin, but in spite of the relatively rapid reduction of retinal in the human retina, Fig. 7 shows that substantial amounts of 468 nm absorbing material still build up and persist for minutes under physiological conditions. This has previously been inferred from in vivo measurements on the human eye (Ripps & Weale, 1969; Alpern, 1971).

The presence of a long lived, visible absorbing intermediate in the human eye makes secondary photoisomerization possible. In the frog retina, photoexcitation of metartiodopsin III has been shown to produce both rhodopsin and isorhodopsin with high quantum yield (Reuter, 1976). Production of rhodopsin is unlikely to have detrimental consequences in the human eye and actually saves the metabolic energy required to chemically regenerate rhodopsin. However, production of isorhodopsin is of interest since the 9-*cis* isomer of retinoic acid is now recognized to be a critical regulator of gene transcription (Kersten, Pan, Chambon, Gronemeyer, & Noy, 1995; Leblanc & Stunnenberg, 1995), and to accelerate rhodopsin expression in postmitotic cells (Wallace & Jensen, 1999). Enzymes have also been shown to exist which specifically oxidize 9-*cis*-retinol to 9-*cis*-retinoic acid (Mertz, Shang, Piantedosi, Wei, Wolgemuth, & Blaner, 1997), making photochemical production of this retinal isomer potentially disruptive to normal cell function. Previously no physiological role has been found for isorhodopsin in nature, but the need to immobilize a potentially toxic substance may account for the evolution of opsins which produce 9-*cis*-pigments. Of course, the amount of 9-*cis*-retinal produced depends critically on the actual intensity and temporal profile of illumination of the retina. However, once this is better established, it becomes important to understand in detail which rhodopsin photointermediates occur and what their photochemical properties are. Finally, we note that extraocular opsins have been proposed to exist in tissues continuously exposed to ambient light. There formation of 9-*cis* retinoids through secondary photolysis might serve in the transduction chain of a circadian oscillator, circumventing the need for the more specialized transduction machinery of the photoreceptor cells.

## Acknowledgements

The authors wish to thank the Montana Eye Bank for its continued effort to make human eyes available for these studies. We also thank the National Institutes of Health for Grant EY-00983 to DSK,FJGMvK was supported by the Air Force Office of Scientific Research, Air Force Systems Command, USAF, under Grant No. 93-NLO36. The US government is authorized to reproduce and distribute reprints for governmental purposes notwithstanding any copyright notation hereon. This research was also in part supported by a Research to Prevent Blindness unrestricted grant.

## References

Alpern, M. (1971). Rhodopsin kinetics in the human eye. *Journal of Physiology*, *217*, 447–471.

Archer, S. N., & Hirano, J. (1998). Rod opsin sequence in the John Dory: further evidence for the spectral tuning of rhodopsin. *Journal of Fish Biology*, *52*, 209–212.

Baumann, C., & Bender, S. (1973). Kinetics of rhodopsin bleaching in the isolated human retina. *Journal of Physiology*, *235*, 761–773.

Baylor, D. A., & Burns, M. E. (1999). Control of rhodopsin activity in vision. *Eye*, *12*, 521–525.

Bennett, N. (1980). Optical study of the light-induced protonation changes associated with the metarhodopsin H intermediate in rod-outer-segment membranes. *European Journal of Biochemistry*, *111*, 99–103.

Blazynski, C., & Ostroy, S. E. (1984). Pathways in the hydrolysis of vertebrate rhodopsin. *Vision Research*, *24*, 459–470.

van Breugel, P. J. G. M., Bovee-Geurts, P. H. M., Bonting, S. L., & Daemen, F. J. M. (1979). Biochemical aspects of the visual process XL. Spectral and chemical aspects of metarhodopsin III in photoreceptor membrane suspensions. *Biochimica et Biophysica Acta*, *557*, 188–198.

Chabre, M., & Breton, J. (1979). The orientation of the chrornophore of vertebrate rhodopsin in the ''meta'' intermediate states and the reversibility of the meta II–meta III transition. *Vision Research*, *19*, 1005–1018.

Crescitelli, F. (1985). Some properties of solubilized human rhodopsin. *Experimental Eye Research*, *40*, 521–535.

Davidson, F. F., Loewen, P. C., & Khorana, H. G. (1994). Structure and function in rhodopsin.6. replacement by alanine of cysteine residues 110 and 187, components of a conserved disuffide bond in rhodopsin, affects the light-activated metarhodopsin II state. *Proceedings of the National Academy of Sciences of the United States of America*, *91*, 4029–4033.

Fasick, L. L., Cronin, T. W, Hunt, D. M., & Robinson, P. R. (1998). The visual pigments of the bottlenose dolphin (*Tursiops truncatus*). *Visual Neuroscience*, *15*, 643–651.

Hendler, R. W., & Shrager, R. I. (1994). Deconvolutions based on singular value decomposition and the pseudoinverse: a guide for beginners. *Journal of Biochemical and Biophysical Methods*, *28*, 1–33.

Hofmann, K. P. (1986). Photoproducts of rhodopsin in the disc membrane. *Photobiochemistry and Photobiophysics*, *13*, 309–327.

Hofmann, K. P., Pulvermüller, A., BuczyIko, L, Van Hooser, P., & Palczewski, K. (1992). The role of arrestin and retinoids in the regeneration pathway of rhodopsin. *The Journal of Biological Chemistry*, *267*, 15701–15706.

Hug, S. J., Lewis, J. W., Einterz, C. M., Thorgeirsson, T. E., & Kliger, D. S. (1990). Nanosecond photolysis of rhodopsin: evidence for a new, blue-shifted intermediate. *Biochemistry*, *29*, 1475–1485.

Jäger, S., Szundi, I., Lewis, J. W., Mah, T. L., & Kliger, D. S. (1998). Effects of pH on rhodopsin photointermediates from lurnirhodopsin to metarhodopsin II. *Biochemistry*, *37*, 6998–7005.

Kersten, S., Pan, L., Chambon, P., Gronemeyer, H., & Noy, N. (1995). Role of ligand in retinoid signaling. 9-*cis*-retinoic acid modulates the oligomeric: state of the retinoid X receptor. *Biochemistry*, *34*, 13717–13721.

Klinger, A. L., & Braiman, M. S. (1992). Structural comparison of metarhodopsin II, metarhodopsin III and opsin based on kinetic

analysis of Fourier transform infrared difference spectra. *Biophysical Journal*, *63*, 1244–1255.

van Kuijk, F. J. G. M., Buck, P., Lewis, J. W., & Kliger, D. S. (1993). Preparative scale isolation and partial purification of human rod outer segments. *Experimental Eye Research*, *57*, 249–252.

Lamb, T. D. (1981). The involvement of rod photoreceptors in dark adaptation. *Vision Research*, *21*, 1773–1782.

Leblanc, B. P., & Stunnenberg, H. G. (1995). *Genes & Development*, *9*, 1811–1816.

Leibrock, C. S., Reuter, T., & Lamb, T. D. (1998). Molecular basis of dark adaptation in rod photoreceptors. *Eye*, *12*, 511–520.

Lewis, J. W., van Kuijk, F. J. G. M., Carruthers, J. A., & Kliger, D. S. (1997). Metarhodopsin III formation and decay kinetics: comparison of bovine and human rhodopsin. *Vision Research*, *37*, 1–8.

Lion, F., Rotmans, J. P., Daemen, F. J. M., & Bonting, S. L. (1975). *Biochimica et Biophysica Acta*, *384*, 283–292.

Mertz, J. R., Shang, E., Piantedosi, R., Wei, S., Wolgemuth, D. J., & Blaner, W. S. (1997). Identification and characterization of a stereospecific human enzyme that catalyzes 9-*cis*-retinal oxidation. *The Journal of Biological Chemistry*, *272*, 11744–11749.

Nagle, J. F., Parodi, L. A., & Lozier, R. H. (1982). Procedure for testing kinetic models of the photocycle of bacteriorhodopsin. *Biophysical Journal*, *38*, 161–174.

Palczewski, K., Jäger, S., BuczyIko, J., Crouch, R. K., Bredberg, D. L., Hofmann, K. P., Asson-Batres, M. A., & Saari, J. C. (1994). Rod outer segment retinol dehydrogenase: Substrate specificity and role in phototransduction. *Biochemistry*, *33*, 13741–13750.

Reuter, T. (1976). Photoregeneration of rhodopsin and isorhodopsin from metarhodopsin III in the frog retina. *Vision Research*, *16*, 909–917.

Ripps, H., & Weale, R. A. (1969). Rhodopsin regeneration in man. *Nature* (*London*), *222*, 775–777.

Rotmans, J. P., Daemen, F. J. M., & Bonting, S. L. (1974). Biochemical aspects of the visual process XXVI. Binding site and migration of retinaldehyde during rhodopsin photolysis. *Biochimica et Biophysica Acta*, *357*, 151–158.

Shrager, R. I., & Hendler, R. W. (1982). Titration of individual components in a mixture with resolution of difference spectra, pKs and redox titrations. *Analytical Chemistry*, *54*, 1147–1152.

Szundi, I., Lewis, J. W., & Kliger, D. S. (1997). Deriving reaction mechanisms from kinetic spectroscopy. Application to late rhodopsin intermediates. *Biophysical Journal*, *73*, 688–702.

Thorgeirsson, T. E., Lewis, J. W., Wallace-Williams, S. E., & Kliger, D. S. (1993). Effects of temperature on rhodopsin photointermediates from lumirhodopsin to metarhodopsin II. *Biochemistry*, *32*, 13861–13872.

Wald, G., & Hubbard, R. (1949). The reduction of retinene, to vitamin $A_1$ in vitro. *Journal of General Physiology*, *32*, 367–389.

Wallace, V. A., & Jensen, A. M. (1999). IBMX, taurine and 9-*cis* retionoic acid all act to accelerate rhodopsin expression in postmitotic cells. *Experimental Eye Research*, *69*, 617–627.

Zvyaga, T. A., Min, K. C., Beck, M., & Sakmar, T. P. (1993). Movement of the retinylidene Schiff base counterion in rhodopsin by one helix turn reverses the pH dependence of the metarhodopsin I to metarhodopsin II transition. *Journal of Biological Chemistry*, *268*, 4661–4667.